THE DIURNAL CYCLE OF TROPOSPHERIC NO_2: CHARACTERIZATION AND IMPLICATIONS FOR THE VALIDATION AND EXPLOITATION OF THE AIR QUALITY SATELLITE CONSTELLATION

T. Verhoelst, C. Gielen, F. Hendrick, J.-F. Müller, G. Pinardi, T. Stavrakou, M. Van Roozendael, and J.-C. Lambert

Royal Belgian Institute for Space Aeronomy (BIRA-IASB), Ringlaan 3, 1180 Brussels, Belgium
Contact: Tijl.Verhoelst@aeronomie.be

ABSTRACT

The tropospheric profile and column abundance of NO_2 and related species represent a key focal point of many current and future satellite missions dedicated to air quality, e.g. those undertaken within the context of the Copernicus Earth observation programme. As these data sets are acquired at different overpass times, photo-chemical changes and potentially also changes in biogenic and anthropogenic emissions will affect any data set intercomparison. To support the validation and synergistic use of these data sets, an in-depth characterization of this diurnal cycle is presented, both from a modelling perspective, using IMAGESv2 CTM data, and using ground-based MAX-DOAS measurements.

1. INTRODUCTION

The tropospheric column abundance of nitrogen dioxide (NO_2) has been measured from space continuously since the pioneering mission GOME was launched in 1995 on board of ESA's ERS-2 mid-morning polar-orbiting satellite: by the mid-afternoon mission EOS-Aura OMI (since 2004) and by the mid-morning missions Envisat SCIAMACHY (2002-2012) and GOME-2 on board of MetOp-A (since 2006) and MetOp-B (since 2012). In the context of the Copernicus Earth observation programme, tropospheric NO_2 will be further monitored by the upcoming afternoon Sentinel-5p TROPOMI, the geostationary MTG-S Sentinel-4, and the mid-morning MetOp-SG Sentinel-5 missions. The validation, intercomparison, and merging of these historical and new datasets, acquired at different solar local times, require advanced colocation methods and ad hoc correction schemes. Indeed, both tropospheric and stratospheric NO_2 concentrations exhibit a pronounced diurnal cycle, primarily of photochemical origin and related to the varying solar zenith angle (SZA), but also affected by intra-day variability of anthropogenic and biogenic emissions (see Fig. 1 for an illustration).

The diurnal cycle of stratospheric NO_2 has been a topic of investigation since the early 70s and 80s using balloon-borne, ground-based, and satellite observations (e.g. Patel et al., 1974; Ridley et al., 1976; Pommereau, 1982; Roscoe et al., 1985). Besides some remaining hurdles regarding OH and aerosol interactions in the lower stratosphere, numerical models nowadays reproduce the stratospheric measurements rather well. Such photochemical models can be used to correct for different overpass times in the intercomparison and validation of satellite measurements of all NO_y species, see for instance Lambert et al. (2004) and Sheese et al. (2016).

In the troposphere, the evolution of NO_2 and related species is further complicated by the surface emissions, which are in fact one of the key targets in air quality research (e.g. Beirle et al., 2003; van der A et al., 2008; Hilboll et al., 2013). The combined use of several (satellite) data sets, their intercomparison, and their validation using ground-based reference measurements will inevitably have to deal with the diurnal cycle of these emissions and their interplay with tropospheric photochemistry (e.g. Blond et al., 2007; Boersma et al., 2008, 2009; Pinardi et al., 2015).

In support to these validation and exploitation activities, we present an in-depth characterization of the diurnal cycle of tropospheric NO_2 and related species, and discuss its impact on data intercomparisons. To this purpose, the tropospheric distribution of nitrogen oxides has been evaluated on a global 2x2.5 degree grid and at high temporal resolution with the IMAGESv2 Chemical Transport Model (CTM) described in Müller and Brasseur (1995) and Stavrakou et al. (2013). Using ERA-interim meteorological fields and extensive emission inventories, IMAGES calculates the evolution of 117 chemical compounds. In Sect. 2, the model output is used to identify distinct regimes, and for each such regime the impact due to differences in solar local time for the above-mentioned missions is discussed. These regimes are mainly related to differences in SZA variation, e.g. polar day versus an equatorial day, and differences in emissions, e.g., unpolluted, forest fires, or urban pollution. To assess the validity of the modeled diurnal cycles, they are compared

Proc. 'Living Planet Symposium 2016', Prague, Czech Republic, 9–13 May 2016 (ESA SP-740, August 2016)

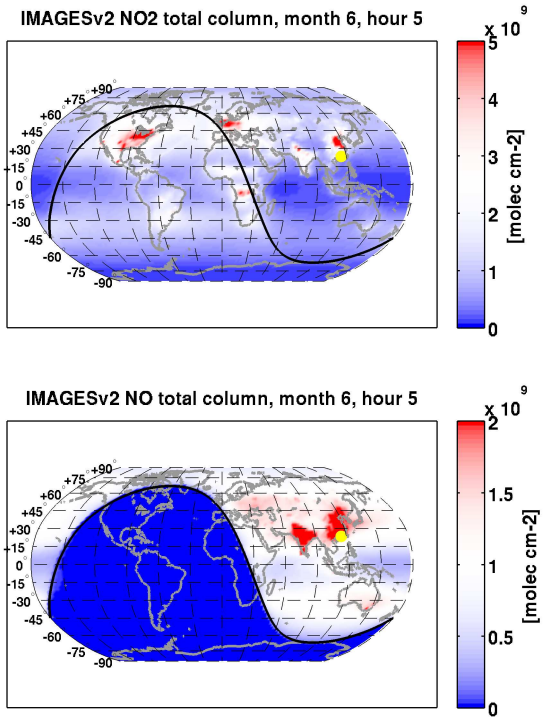

Figure 1. NO_2 (upper panel) and NO (lower panel) columns up to approx. 20km as simulated with the IMAGESv2 CTM, illustrating the impact of both photochemistry and local anthropogenic and biogenic emissions. The black line represents the terminator, the yellow dot the subsolar point. NO is only present during daytime, from photodissociation of NO_2. Emission hot spots, either industrial (e.g. Western Europe, around the Great Lakes in the US, from Beijing to Shanghai in China) or biogenic (e.g. central Africa) are also clearly present.

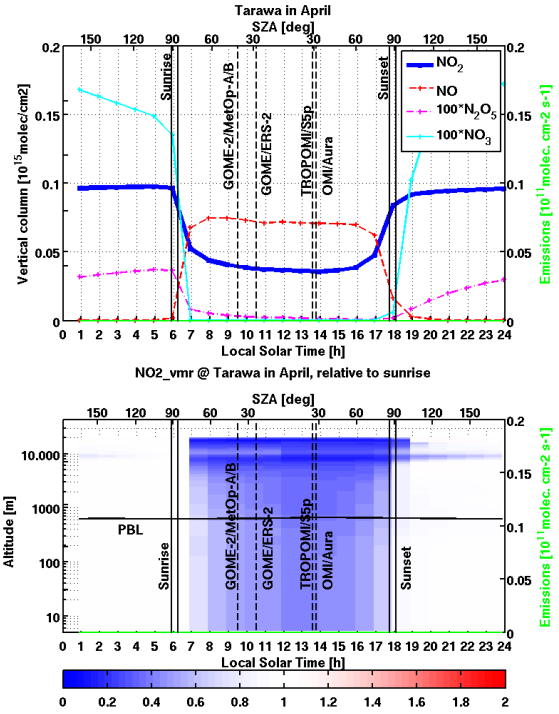

Figure 2. **Upper panel:** *Diurnal cycle of the tropospheric column of NO_2 and related species at the equatorial site of Tarawa (1°N, 173°E), an atoll in the central Pacific Ocean. Sunrise and sunset conditions are marked, and so are the overpass times of several key air quality satellite sounders. The bright green curve (right-hand axis) represents the combined NO_x emissions, both anthropogenic and biogenic, which are in this case negligible.* **Lower panel:** *Diurnal cycle of the concentration (volume mixing ratio, VMR) of NO_2 as a function of altitude and normalized to the value at sunrise. The border of the planetary boundary layer (PBL) is indicated.*

in Sect. 3 to ground-based MAX-DOAS UV-visible measurements at selected sites representing both rural and urban conditions.

2. IDENTIFYING DIFFERENT REGIMES IN CTM DATA

In the following, the diurnal evolution of NO_2 and related species as captured by the IMAGESv2 CTM is illustrated for 4 different locations, representing several key regimes and their distinctive features. These cover both differences in illumination (SZA variation throughout the day) and in surface emissions (rural, urban,...).

2.1. Equatorial and unpolluted:

A first case study concerns an unpolluted equatorial site in local spring, for instance the Tarawa atoll (1°N, 173°E), part of Kiribati in the central Pacific Ocean. The total tropospheric column for NO_2 and related species is shown in the upper panel of Fig. 2. NO_2, NO_3, and N_2O_5 suffer strong photolysis at sunrise, which for N_2O_5 continues throughout the day. At sunset, noctural levels are restored roughly within an hour, except for the N_2O_5 column which continues to rise throughout the night. For NO and NO_2, daytime and nighttime columns are stable to within a few percent. This behaviour is unlike that in the stratosphere, where a reaction involving either O_3 or ClO leads to a steady increase of NO_2 during daytime, at the expense of the NO column. The bottom panel of Fig. 2 reveals that the evolution of NO_2 concentrations is independent of altitude, both in the Planetary Boundary Layer (PBL) and free troposphere.

From these results, it is clear that the different overpass times of the satellite missions considered here should not lead to significantly different column or concentration measurements in this particular atmospheric regime, except for N_2O_5, for which the column decreases slowly

during the day. Comparison with ground-based (MAX-DOAS) measurements during twilight on the other hand would require the application of a correction scheme, although in practice tropospheric measurements are usually only made up to 85° SZA, beyond which the observing mode is switched to zenith-sky (stratospheric) measurements. Note also that the NO_2 columns described here are below the detection limit of the current generation of satellite sounders (typically $1e15$ molec cm^{-2}).

2.2. High latitude and unpolluted:

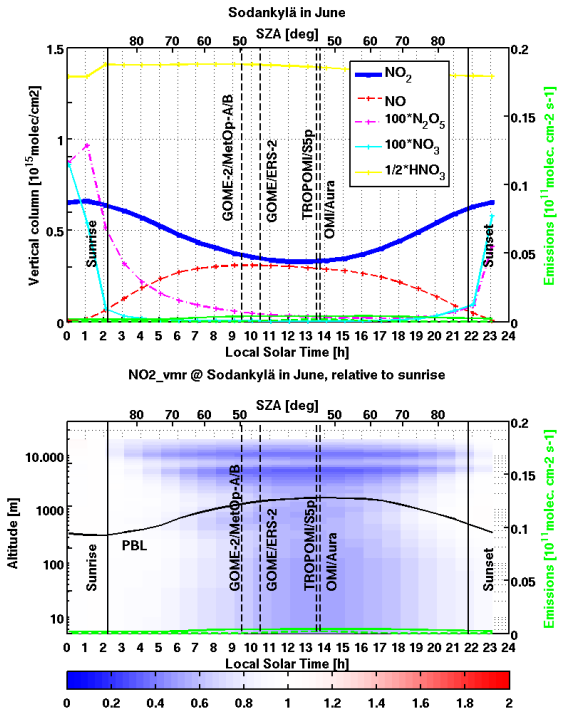

Figure 3. Similar to Fig. 2 but for the high-latitude rural site of Sodankylä (67°N, 26°E), located in Finland close to the Arctic Circle. The chosen date corresponds to the polar day regime, i.e. sunrise and sunset merge into one twilight period, with the sun never actually disappearing below the horizon.

The second example, shown in Fig. 3 represents a high-latitude location during polar day. Similar to what is known for the stratospheric diurnal cycle, the absence of a daily period of darkness and the slow SZA evolution throughout the day, lead to a very smooth evolution in NO_x columns and concentrations. The bottom panel of Fig. 3 illustrates how higher atmospheric layers experience a more pronounced cycle due to a decreased daytime conversion of NO to NO_2 by reaction with O_3, a reaction with a six-fold lower rate at 220 K compared to 298 K.

Depending on the measurement uncertainty and scientific objectives, different overpass times may lead to differences in observed columns and concentrations that need to be taken into account in a comparative or synergistic analysis.

2.3. High latitude with biogenic emissions

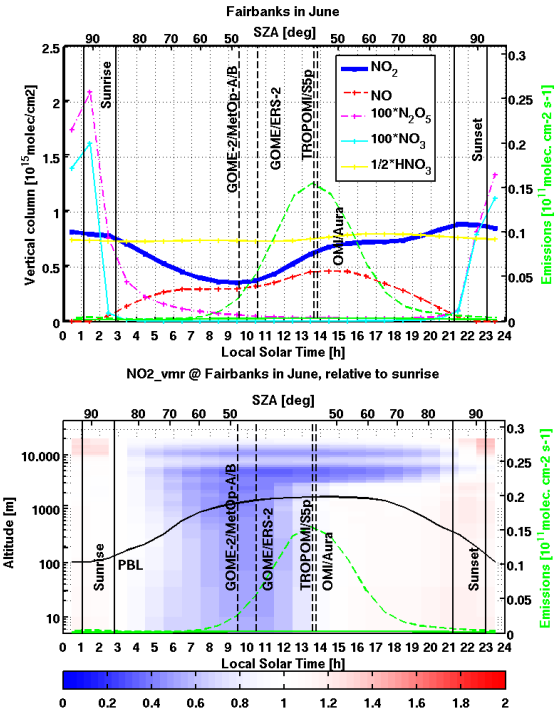

Figure 4. Similar to Fig. 2 but for the high-latitude site of Fairbanks (65°N, 148°W), at a time of significant forest fires.

The next example (Fig. 4) also deals with a high-latitude site (Fairbanks, Alaska, located 65°N, 148°W) close to polar day, but contrary to the case study at Sodankylä, this one is characterized by biogenic NO_x emissions from strong forest fires, which are known to peak in the afternoon. These emissions are clearly visible around the OMI/Aura and TROPOMI/S5p overpass times, in both the NO_2 and NO columns. The bottom panel of Fig. 4 confirms that the emissions only affect the altitudes below the maximum altitude of the PBL, as expected. In the free troposphere, the behaviour is very similar to the unpolluted case at Sodankylä.

It is very clear here that different overpass times will imply different sensitivity to the afternoon emissions, at least for measurements sensitive to the concentrations in the PBL.

2.4. Mid latitude with anthropogenic emissions

The final example, shown in Fig. 5 and dealing with a winter day at the urban site of Uccle (51°N, 4°E)

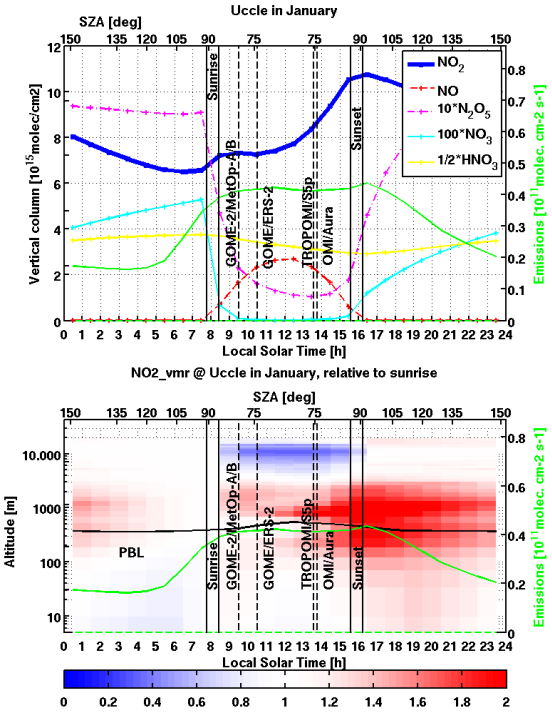

Figure 5. Similar to Fig. 2 but for the mid-latitude urban site of Uccle (51°N, 4°E) , close to Brussels, Belgium.

near Brussels, Belgium, represents the most complex case, with significant anthropogenic NO_x emissions during daytime. While a mid-latitude rural (unpolluted) site would be characterized by a sharp decrease and increase of NO_2 at sunrise and sunset respectively (somewhat similar to Fig. 2) this photo-chemical loss during daytime is here completely filled in by the emissions. Only well into the free troposphere (around 10 km altitude) does the behaviour resemble that of an unpolluted regime (see bottom panel of Fig. 5). In fact, quite striking and requiring further investigation is the apparent increase in NO_2 concentrations also above the PBL. This is at odds with the expectation that mostly vertical mixing within the PBL brings the emissions to higher altitudes. Note that in the previous case study (Fig. 4), the impact of the emissions was clearly limited to the PBL, as expected.

Again, different overpass times will lead to substantially different column and concentration measurements, from the surface up to at least several km. In fact, NO_2 changes during the afternoon and NO changes from sunrise to sunset occur so rapid that also the co-location with e.g. ground-based MAX-DOAS measurements will require very strict time constraints.

3. COMPARISON WITH MAX-DOAS MEASUREMENTS

To assess the validity of the IMAGESv2 modelled diurnal cycles of NO_2, they were compared to ground-based MAX-DOAS UV-visible measurements at two sites, representing either rural or urban conditions. For the present study, only tropospheric columns were looked at, i.e. profile comparisons are still to be done. Also, the MAX-DOAS vertical averaging kernels were not yet used to properly weight the model profiles when computing the IMAGESv2 column counterparts. When the model profile is not too different from the a priori used in the MAX-DOAS retrieval at those altitudes where measurement sensitivity is low, the impact of this simplification will be minor. A case where this assumption probably is not met, is discussed in Sect. 3.2.

In order to reveal the average diurnal cycle at first hidden in the day-to-day variability and measurement noise, the MAX-DOAS measurements were binned by season and by hour in local solar time (LST).

Shown here are results for the MAX-DOAS instruments operated at the Observatoire de Haute Provence (OHP), France, and in Uccle, Belgium. From the former, roughly 52000 measurements are available, covering the period from June 2006 to December 2015. For the latter, a more limited 3000 measurements remain after cloud filtering, covering the period from April 2011 until December 2015. See Valks et al. (2011) and Gielen et al. (2014) respectively for more details on the instruments and retrieval methods.

3.1. A rural site: OHP

The Observatoire de Haute Provence can be considered a rural site, only occasionally affected by the transport of pollution from regional sources (e.g. from the petrochemical plants of Etang de Berre close to Marseille), and with only minor anthropogenic emissions taken into account in the IMAGESv2 model, following the emissions inventory (at most 1e10 molec. cm^{-2} s^{-1}). The diurnal cycle is clearly visible in the MAX-DOAS data, with little variation across the year, besides the change in length of day. In spring and summer the IMAGESv2 simulation matches the observed curves fairly well, albeit with some underestimation, in particular near twilight. In late autumn and winter, the observed curve is somewhat different, with larger than expected columns at and after noon. Given the similarity with the steady increase of NO_2 columns during daytime at Uccle (see next Section), this could point at too low an estimate for the emissions term, potentially due to differences in horizontal sensitivity between the model and the MAX-DOAS measurements.

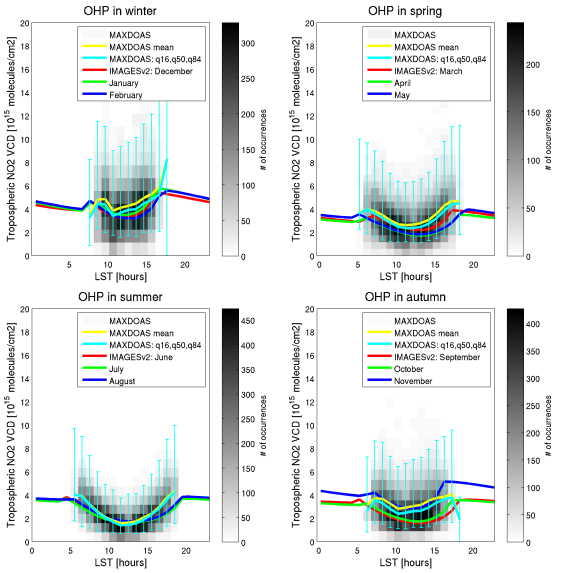

Figure 6. Diurnal cycle of the tropospheric NO_2 column, both measured (MAX-DOAS) and modelled (IMAGESv2), at the Observatoire de Haute Provence in Southern France (44°N, 6°E). The grey-scale background represents the density of the MAX-DOAS measurements, binned per season and hour (LST). Dark regions represent very common NO_2 column values, lighter regions correspond to less frequently observed values.

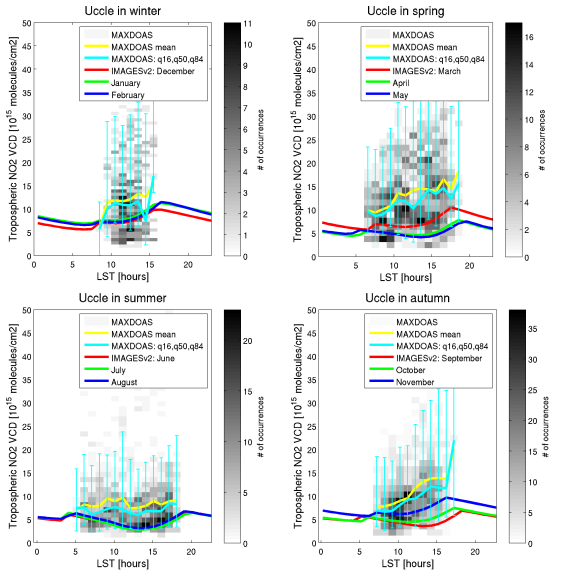

Figure 7. Similar to Fig. 6 but for the urban site of Uccle, Belgium. Note the different scale, to accomodate the much larger NO_2 levels.

3.2. An urban site: Uccle

As already discussed in Sect. 2.4, Uccle is a complex case where the diurnal cycle can be significantly affected by anthropogenic emissions, in particular in winter. Moreover, the mini-MAX-DOAS points North, to the center of Brussels. Figure 7 reveals clear diurnal variations. More specifically, autumn, winter, and spring are characterized by increasing NO_2 columns throughout the day, very similar to the behaviour of the IMAGESv2 data presented in Fig. 5. The summer-time MAX-DOAS data show a more flat behaviour, but this represents an excess w.r.t. the almost "rural" modelled curves. Moreover, the model generally underestimates the observed columns. This is likely due to differences in horizontal resolution: The model grid cells measure $2.5° \times 2°$ in longitude and latitude, covering almost all of Belgium, while the MAX-DOAS measurements have a very confined sensitivity near Brussels. Also, in this particular case, applying the MAX-DOAS vertical averaging kernels to the model profile before computing the tropospheric column may further reduce the model columns, as some part of the afternoon NO_2 increase in the model occurs fairly high up, where the MAX-DOAS sensitivity is lower than at the surface. Further investigation, including profile comparisons, is clearly required.

4. CONCLUSIONS AND PROSPECTS

In this exploratory study, CTM data were generated, analyzed, and compared to MAX-DOAS measurements with a focus on the diurnal cycle of tropospheric NO_2 and related species. In contrast to the mostly photo-chemical evolution of these species in the stratosphere, the diurnal cycle in the troposphere, and in particular in the planetary boundary layer, can be heavily affected by anthropogenic and biogenic emissions. For instance, in an urban environment, daytime emissions can overcompensate the photochemical loss of NO_2. Qualitatively, these results are confirmed by the MAX-DOAS measurements, although differences in horizontal and vertical sensitivity complicate the intercomparison. Except for a few specific situations, e.g. in unpolluted equatorial regions, different overpass times will lead to substantially different NO_x column and concentration measurements. Transfer schemes, to be applied both for the validation and synergistic use of current and future air quality satellite data sets, need to be developed, and CTM data could contribute to this.

ACKNOWLEDGMENTS

This work was funded by the Belgian federal Science Policy Office (BELSPO) through the PRODEX project AcroSat (*http://tropo.aeronomie.be/acrosat/index.htm*).

REFERENCES

Beirle, S., Platt, U., Wenig, M., and Wagner, T. (2003). Weekly cycle of NO2 by GOME measurements: a signature of anthropogenic sources. Atmos. Chem. Phys., 3(6):2225–2232.

Blond, N., Boersma, K. F., Eskes, H. J., van der A, R. J., Van Roozendael, M., De Smedt, I., Bergametti, G., and Vautard, R. (2007). Intercomparison of SCIAMACHY nitrogen dioxide observations, in situ measurements and air quality modeling results over western Europe. Journal of Geophysical Research, 112(D10).

Boersma, K. F., Jacob, D. J., Eskes, H. J., Pinder, R. W., Wang, J., and van der A, R. J. (2008). Intercomparison of SCIAMACHY and OMI tropospheric NO2 columns: Observing the diurnal evolution of chemistry and emissions from space. J. Geophys. Res., 113(D16).

Boersma, K. F., Jacob, D. J., Trainic, M., Rudich, Y., DeSmedt, I., Dirksen, R., and Eskes, H. J. (2009). Validation of urban NO2 concentrations and their diurnal and seasonal variations observed from the SCIAMACHY and OMI sensors using in situ surface measurements in Israeli cities. Atmos. Chem. Phys., 9(12):3867–3879.

Gielen, C., Van Roozendael, M., Hendrick, F., Pinardi, G., Vlemmix, T., De Bock, V., De Backer, H., Fayt, C., Hermans, C., Gillotay, D., and Wang, P. (2014). A simple and versatile cloud-screening method for max-doas retrievals. Atmospheric Measurement Techniques, 7(10):3509–3527.

Hilboll, A., Richter, A., and Burrows, J. P. (2013). Long-term changes of tropospheric NO2 over megacities derived from multiple satellite instruments. Atmos. Chem. Phys., 13(8):41454169.

Lambert, J.-C. et al. (2004). Geophysical Validation of SCIAMACHY NO2 Vertical Columns: Overview of Early 2004 Results. In Proceedings of the Second Workshop on the Atmospheric Chemistry Validation of ENVISAT (ACVE-2). ESA-ESRIN, Frascati, Italy.

Müller, J.-F. and Brasseur, G. (1995). Images: A three-dimensional chemical transport model of the global troposphere. Journal of Geophysical Research, 100(D8):16445.

Patel, C., Burkhardt, E., and Lambert, C. (1974). Spectroscopic measurements of nitric oxyde and water vapor. Science, 184:1173–1176.

Pinardi, G., Lambert, J.-C., Yu, H., Smedt, I. D., Granville, J., Roozendael, M. V., and Valks, P. (2015). O3M SAF VALIDATION REPORT. Technical Report SAF/O3M/IASB/VR/NO2, BIRA-IASB.

Pommereau, J. P. (1982). Observation of NO2 diurnal variation in the stratosphere. Geophysical Research Letters, 9(8):850–853.

Ridley, B., Bruin, J., Schiff, H., and McConnell, J. (1976). Altitude profile and sunset decay measurements of stratospheric nitric oxide. Atmosphere, 14(3):180–188.

Roscoe, H. K., Kerridge, B. J., Gray, L. J., Wells, R. J., and Pyle, J. A. (1985). In Zerefos, C. S. and Ghazi, A., editors, Atmospheric Ozone: Proceedings of the Quadrennial Ozone Symposium held in Halkidiki, Greece 3–7 September 1984, pages 173–174, Dordrecht. Springer Netherlands.

Sheese, P. E., Walker, K. A., Boone, C. D., McLinden, C. A., Bernath, P. F., Bourassa, A. E., Burrows, J. P., Degenstein, D. A., Funke, B., Fussen, D., and et al. (2016). Validation of ACE-FTS version 3.5 NOy species profiles using correlative satellite measurements. Atmospheric Measurement Techniques Discussions, pages 1–55.

Stavrakou, T., Müller, J.-F., Boersma, K. F., van der A, R. J., Kurokawa, J., Ohara, T., and Zhang, Q. (2013). Key chemical NOx sink uncertainties and how they influence top-down emissions of nitrogen oxides. Atmospheric Chemistry and Physics, 13(17):9057–9082.

Valks, P., Pinardi, G., Richter, A., Lambert, J.-C., Hao, N., Loyola, D., Van Roozendael, M., and Emmadi, S. (2011). Operational total and tropospheric NO2 column retrieval for GOME-2. Atmos. Meas. Tech., 4(7):1491–1514.

van der A, R. J., Eskes, H. J., Boersma, K. F., van Noije, T. P. C., Van Roozendael, M., De Smedt, I., Peters, D. H. M. U., and Meijer, E. W. (2008). Trends, seasonal variability and dominant NOx source derived from a ten year record of NO2 measured from space. Journal of Geophysical Research, 113(D4).